

UCSF

UC San Francisco Previously Published Works

Title

Dynamic imaging demonstrates that pulsed electromagnetic fields (PEMF) suppress IL-6 transcription in bovine nucleus pulposus cells

Permalink

<https://escholarship.org/uc/item/3w82m2gw>

Journal

Journal of Orthopaedic Research®, 36(2)

ISSN

0736-0266

Authors

Tang, Xinyan
Alliston, Tamara
Coughlin, Dezba
[et al.](#)

Publication Date

2018-02-01

DOI

10.1002/jor.23713

Copyright Information

This work is made available under the terms of a Creative Commons Attribution License, available at <https://creativecommons.org/licenses/by/4.0/>

Peer reviewed

Dynamic Imaging Demonstrates That Pulsed Electromagnetic Fields (PEMF) Suppress IL-6 Transcription in Bovine Nucleus Pulposus Cells

Xinyan Tang,¹ Tamara Alliston,¹ Dezba Coughlin,¹ Stephanie Miller,¹ Nianli Zhang,² Erik I. Waldorff,² James T. Ryaby,² Jeffrey C. Lotz¹

¹Department of Orthopaedic Surgery, University of California San Francisco, San Francisco, California, ²Orthofix Inc., Lewisville 75056 Texas

Received 7 April 2017; accepted 19 August 2017

Published online 19 August 2017 in Wiley Online Library (wileyonlinelibrary.com). DOI 10.1002/jor.23713

ABSTRACT: Inflammatory cytokines play a dominant role in the pathogenesis of disc degeneration. Pulsed electromagnetic fields (PEMF) are noninvasive biophysical stimulus that has been used extensively in the orthopaedic field for many years. However, the specific cellular responses and mechanisms involved are still unclear. The objective of this study was to assess the time-dependent PEMF effects on pro-inflammatory factor IL-6 expression in disc nucleus pulposus cells using a novel green fluorescence protein (GFP) reporter system. An MS2-tagged GFP reporter system driven by IL-6 promoter was constructed to visualize PEMF treatment effect on IL-6 transcription in single living cells. IL-6-MS2 reporter-labeled cells were treated with IL-1 α to mimic the in situ inflammatory environment of degenerative disc while simultaneously exposed to PEMF continuously for 4 h. Time-lapse imaging was recorded using a confocal microscope to track dynamic IL-6 transcription activity that was demonstrated by GFP. Finally, real-time RT-PCR was performed to confirm the imaging data. Live cell imaging demonstrated that pro-inflammatory factor IL-1 α significantly promoted IL-6 transcription over time as compared with DMEM basal medium condition. Imaging and PCR data demonstrated that the inductive effect of IL-1 α on IL-6 expression could be significantly inhibited by PEMF treatment in a time-dependent manner (early as 2 h of stimulus initiation). Our data suggest that PEMF may have a role in the clinical management of patients with chronic low back pain. Furthermore, this study shows that the MS2-tagged GFP reporter system is a useful tool for visualizing the dynamic events of mechanobiology in musculoskeletal research. © 2017 The Authors. *Journal of Orthopaedic Research*® Published by Wiley Periodicals, Inc. on behalf of Orthopaedic Research Society. *J Orthop Res* 35:778–787, 2018.

Keywords: MS2-GFP reporter; dynamic imaging; pulsed electromagnetic fields; IL-6 mRNA expression; spine/disc biology

Intervertebral disc (IVD) degeneration is ubiquitous in the adult population and associates with back pain-related disabilities.¹ Low back pain causes more disability globally than any other conditions, and creates a significant financial burden on the worldwide health care system (>\$100 billion per year).^{2,3} Disc degeneration occurs when undesired cell behaviors, particularly the imbalanced secretion of the anabolic, and catabolic factors, triggers degradation of extracellular matrix, leading to a series of inflammatory responses and further cell dysfunction.^{4–7} Due to the disc's poor capability of self-regeneration, many strategies have been developed to promote tissue repair that include stem cell, growth factor, and biomaterial approaches.^{8–9} Unfortunately, these approaches have not yet been successfully translated to the clinic, likely because the microenvironment within degenerated disc hinders their therapeutic effects. Therefore, there is a pressing need for therapeutic approaches that reestablish tissue homeostasis and reverse the catabolic cell behaviors underlying painful disc degeneration.

Pro-inflammatory cytokines and inflammatory mediators play crucial roles in the initiation and

progression of disc degeneration. These include interleukins (IL-1, IL-2, IL-6, IL-8, and IL-17), interferon gamma (IFN- γ), TNF- α , nitric oxide (NO), and prostaglandin E2 (PGE2),^{10–12} which are elevated in the degenerated NP and annulus fibrosus (AF), and associate with matrix degradation.^{12–13} Among these factors, IL-1 plays a predominant role by up-regulating the expression of IL-6, IL-17, MMP3/13, ADAMTSs, iNOS, Cox-2, PGE2, and by inhibiting anabolic factor production.^{11,12,14–18} Ultimately, these undesired cell behaviors frustrate therapeutic strategies for disc regeneration.

PEMF is a noninvasive biophysical stimulation that has been used clinically for enhancing bone healing and treating failed fusions, pseudoarthrosis, and osteoporosis.^{19–23} Positive clinical outcomes have inspired researchers to explore PEMF mechanisms so as to further optimize current treatments and expand clinical indications. Recently, several in vitro studies have shown that PEMF could promote cartilage and bone metabolism by stimulating chondrocyte/osteoblast/tendon cell proliferation and differentiation, and by positively modulating matrix synthesis.^{24–29} Additionally, PEMF has been implicated in inflammatory response modulation. For example, PEMF treatment can reduce the secretion of pro-inflammatory cytokine IL-1 β and TNF- α in fibroblast-like cell, decrease IL-6/IL-8 release in lymphocytes from rheumatoid arthritis patient,^{30,31} inhibit PGE2, and vascular endothelial growth factor (VEGF) secretion in chondrocytes,³² promote anti-inflammatory cytokine factors release, and preserve cartilage/disc tissue from detrimental environment of high inflammatory cytokine levels

This is an open access article under the terms of the Creative Commons Attribution License, which permits use, distribution and reproduction in any medium, provided the original work is properly cited.

Conflict of interest: None

Grant sponsor: Orthofix Inc..

Correspondence to: Jeffrey C. Lotz (T: +415-476-7881;

F: (415-476-1128; E-mail: jeffrey.lotz@ucsf.edu)

© 2017 The Authors. *Journal of Orthopaedic Research*® Published by Wiley Periodicals, Inc. on behalf of the Orthopaedic Research Society.

during degeneration.^{30,32–34} Taken together, these studies suggest that an important therapeutic activity of PEMF is the regulation of cell inflammatory behaviors. Our previous study indicated that PEMF stimulation could significantly reduce pro-inflammatory cytokine IL-6 expression in the presence of IL-1 α in human degenerated disc cells at day 4.³⁵ This was the first evidence that PEMF can modulate acute inflammatory behaviors of disc cells that associate with chronic discogenic back pain. However, the temporal and spatial resolution of cellular responses and molecular events involved with PEMF are still poorly understood. Moreover, the underlying mechanisms of PEMF action remains unclear. Studying these cellular and molecular responses will help to elucidate mechanism and optimize PEMF treatment conditions such as pulse intensity, frequency, and dosing time to maximize clinical benefits.

For evaluating the dynamic effect of PEMF on IL-6 transcription, a newly developed technology, GFP-tagged MS2 reporter system,^{36–40} was adopted to visualize in real time the transactivation of the IL-6 gene through tracking GFP produced in single living cells in vitro. This technology allows a GFP-MS2 fusion protein (expressed by the first plasmid) to specifically bind to the RNA motif containing MS2 repeat sequence (expressed by the second plasmid), therefore resulting in an amplified, bright green fluorescent particles in cells (Fig. 1). By visualizing the bright GFP particle activity, dynamic transactivation of a specific mRNA can be traced within the cell. This system has been confirmed by many in vitro studies, and has even been applied in vivo.^{37,38,41–44} In the present study, MS2-tagged GFP system was the first time applied in musculoskeletal tissues to visualize and evaluate dynamic effects of PEMF treatment on IL-6 transcriptional activity in bovine NP cells. The

data will help to optimize PEMF treatment conditions therefore benefit clinical treatment.

METHODS

The GFP-MS2 and Reporter Expressing Vectors

Two key constructs were used in this study: Plasmid A is an MS2-GFP fusion protein (PGK-MS2-GFP). Plasmid B is a reporter mRNA (IL-6-RFP-MS2 \times 24 binding sites). Together they comprise a novel application of the previously described MS2-tagged GFP system, adapted here to evaluate the dynamic regulation of IL-6.^{38,39,43,44} Plasmid A: the MS2-GFP fusion construct was made by excising the MS2-GFP-NLS from pMS2-GFP (Addgene, Cambridge, MA) with NheI and ClaI sites and ligating in between NotI and HindIII sites of p miniTol2 (Addgene). Plasmid B: the mRNA reporter construct was generated by ligating IL-6 promoter-RFP-MS2 \times 24 in between NotI and HindIII sites of p miniTol2 (Addgene). MS2 \times 24 sequence was synthesized by Invitrogen (CA). The two constructs were validated via gene sequencing (MCLab, CA). In this reporter system, the fluorescent signal is amplified through recruitment of the MS2-GFP fusion protein to the 24 MS2-binding motifs in the reporter mRNA, which is expressed under control of the IL-6 promoter. When bound to the reporter, the MS2-GFP fusion protein forms bright nuclear GFP particles, such that the number and intensity of fluorescent particles corresponds to the level of IL-6 mRNA induction. The schematics of constructs are described in Figure 1.

Cell Culture and Transfection

IVDs were harvested from bovine caudal spines (18–24 month old). The discs were dissected and separated into zones of annulus fibrosis (AF) and nucleus pulposus (NP) according to their distinct morphological appearance where AF is a highly dehydrated lamellar structure while NP is a gelatinous structure. After digestion in a protease/collagenase cocktail overnight, retrieved NP cells were suspended in Basal Media (low-glucose Dulbecco's Modified Eagle's media (DMEM) (Invitrogen Life Technologies, Carlsbad, CA) supplemented with 5% fetal bovine serum (FBS,

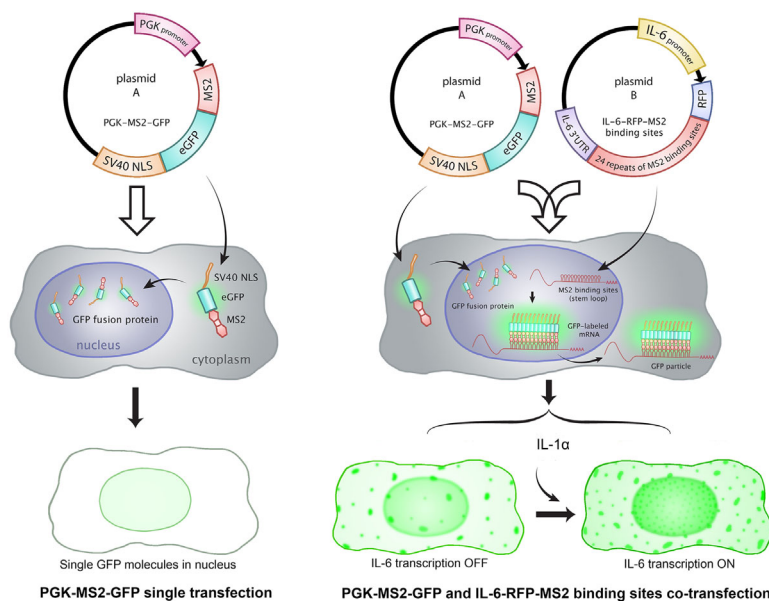


Figure 1. Schematic of MS2 constructs used in this study. Plasmid A) PGK-MS2-GFP fusion protein Plasmid, expresses the MS2-GFP fusion protein; Plasmid B) reporter mRNA, expresses an MS2 \times 24 repeat sequence driven by IL-6 promoter (IL-6-RFP-MS2). Single transfected cells (Plasmid A, left side) showed a diffuse green fluorescence concentrated within the cell nucleus because of the nuclear localization sequence (NLS); In co-transfected cells (right side), the fusion protein co-expresses with the reporter mRNA containing MS2-binding sites. The fusion protein specifically binds to one of the 24 copies of the RNA motif contained in the MS2 \times 24 repeat sequence. The resultant binding of multiple copies of the MS2-GFP fusion protein to the mRNA forms bright green particles in cells (particularly induced by pro-inflammatory factor IL-1 α).

HyClone, South Logan, UT), non-essential amino acids solution (Invitrogen), antibiotic/antimycotic (100 U/ml penicillin, 100 µg/ml streptomycin, and 0.25 µg/ml fungizone, Invitrogen), 1.5% osmolarity salt solution (containing 5 M NaCl and 0.4 M KCl, Sigma, St. Louis, MO). Cells were cultured in an incubator at 37°C with 5% CO₂ and 95% humidity, and expanded to passage two for these experiments.

Transfections were performed with electroporation (10 µg DNA, Neon[®] Transfection System, Life Technologies) when cells reached 70–80% confluence.

Flow Cytometry

To verify the MS2-GFP reporter system, flow cytometry was used to detect the expression of red fluorescence protein (RFP) and GFP. Cells were transfected with either of the two plasmids (pMS2-GFP or pIL-6-RFP-MS2 × 24) alone or in combination. After culture for 36 h trypsinized cells were used to quantify the expression of GFP and RFP. Unlabeled cells were chosen as a negative control for gating the target cell population base on cell size, shape and optical homogeneity, and setting the fluorescence threshold for quantifying positive cells (GFP and RFP positive). The percentage of fluorescence-positive cells and mean fluorescence intensity (MFI) were analyzed using a BD Fortessa flow cytometer at 488 and 561 nm wavelength. Each group has three biological replicates for flow cytometry analysis.

Pulse Electronic Magnetic Field (PEMF) Setting

The PEMF device used in this study has similar waveform parameters as the clinically-approved Physio-Stim[®] PEMF device for treatment of long bone non-unions (Orthofix Inc., Lewisville, TX). Specifically the electromagnetic waveform was a triangular wave with a 25% duty cycle, 3,850 Hz pulse frequency, 15 Hz burst frequency, and maximum 10 T/s rate of change. The PEMF exposure system itself consisted of a coil fitted to a confocal microscope, with a diameter large enough to hold a 35 mm diameter dish during exposure. To ensure uniform exposure a dB/dt sensor was used to monitor the magnetic field during PEMF treatment.

Real-Time Reverse Transcription PCR

To understand cellular responses to PEMF, real time quantitative PCR (qRT-PCR) was used to assay gene expression after PEMF treatment. Cells grown in DMEM Basal Medium were divided into three groups: DMEM Basal Medium group, IL-1α treatment group (10 ng/ml), and IL-1α +PEMF treatment group. PEMF was turned on after 2 h of IL-1α treatment, and both PEMF and IL-1α were used continuously to treat cells for 4 h beyond that. Cell samples were collected at 1, 3, 4, 6, and up to 8 h after initiation of IL-1α treatment for RNA isolation and cDNA synthesis (Qiagen, Valencia, CA). cDNA was amplified with specific primers for bovine IL-6 (Forward: TGAGTGTGAAAGCAGCAAGGA; Reverse: TACTCCAGAAGACCAGCAGTGG) and GAPDH (Forward: GCCATCACTGCCACCCAGAA; Reverse: GCGGCAGGTCAGATCCACAA) using the iQ SYBR Green Supermix kit (BioRad, Hercules, CA). Real time PCR was performed with the iCycler iQ system (BioRad, Hercules). Bovine GAPDH was selected as the internal reference. Each group has three biological replicates, each of which had three technical replicates. Relative gene expression was determined using the delta-delta CT method.⁴⁵

Confocal Microscopy, Live-Cell Imaging, and Analysis

For live imaging, transfected cells were cultured in 35 mm glass-bottom tissue-culture dishes (MatTek, Ashland, MA). The glass bottom was pre-coated with collagen type I solution, 50 µg/ml (BD Bioscience, Tewksbury, MA) at 4°C overnight. Transfected cells were cultured for 36–40 h prior to imaging using confocal laser point scanning microscope (Leica, TCS SP5, Mannheim, Germany). To maintain 37°C, 5% CO₂, and 95% humidified atmosphere throughout imaging, the microscope was equipped with a temperature control cube (Life Imaging Services, Basel, Switzerland), with CO₂ and humidity control (OkoLab, Pozzuoli, NA, Italy). Time-lapse imaging in four dimensions (X, Y, Z over time) was recorded with 12 bit camera at 400 Hz speed using a HC PL APO 63×/1.40 objective (Leica, Mannheim, Germany). GFP fluorescence was detected using an Argon Laser (488 nm, 20% output) with 8–10% laser power. Mark and Find function was used to record multiple cell positions every half hour, and the z-slice thickness was maintained at ~0.5 µm. During imaging, cells were treated with DMEM media with or without IL-1α (10 ng/ml, GenScript, NJ) for 2 h prior to administration of PEMF for 4 h (IL-1α was present together with PEMF during the whole experiment).

Imaris software (Bitplane, MA) was used to analyze the images captured on the confocal microscope. With the tracking module of Imaris, the GFP particles within a 3D volume of the cells were counted, tracked, and analyzed according to the threshold of particle size (0.5 µm) and of intensity.

Statistical Analysis

Statistical differences were tested using a one-way analysis of variance (ANOVA), followed by Fisher's PLSD for comparing multiple groups. All analyses were performed using StatView 5.0 (SAS institute, Inc. Cary, NC). Data are depicted as mean ± 95% confidence intervals, and *p*-values less than 0.05 were considered significant.

Biological replicates represent unique bovine tails. Three biological replicates were used for flow cytometry and PCR studies. Technical replicates for RNA represent unique wells of cells in independent experiments as well as triplicate wells in qPCR analysis. For imaging, only one tail was used. At least three independent experiments were performed for each group and technical replicates (*n* = 9) represent the cells.

RESULTS

Inductive Effects of Pro-Inflammatory Cytokine IL-1α on IL-6 Gene Expression

Expression of IL-6 in bovine nucleus pulposus cells was measured using real-time qRT-PCR. In basal medium, IL-6 expression was low over time in NP cells (Fig. 6). However, after IL-1α treatment, IL-6 expression significantly increased in a time-dependent manner from 3 h (*p* = 0.07) to 8 h (*p* < 0.01). Note: The time points mean the time after initiation of IL-α treatment.

Expression of the MS2-GFP Reporter in Nucleus Pulposus Cells

The effect of IL-1α on IL-6 expression inspired us to trace the dynamic expression of IL-6. When transfected

only with Plasmid A, the MS2-GFP fusion protein is confined to the nucleus because of the nuclear-localization sequence in MS2-GFP fusion protein. When Plasmid A is cotransfected with Plasmid B, some bright green GFP particles are apparent due to the specific recruitment of the MS2-GFP fusion protein to the binding sites upon basal expression of the mRNA reporter (Fig. 1; Fig. 2A). After induction by IL-1 α treatment (“IL-6 ON”) compared with “OFF” state (without IL-1 α), many more bright green GFP particles were rapidly produced (Fig. 2A2). These GFP particles were distributed within both the nucleus and cytoplasm (Fig. 2B). Of these, particles with the strongest intensity were found in the nucleus due to the accumulation of enriched GFP molecule in the nucleus. Therefore, GFP-bound mRNA presented as bright green particles interspersed within a diffuse, lower intensity signal in cells (Fig. 2A2), which is similar to the data reported in previous studies.^{37,38,43,44,46,47} Interestingly, the particle shape is not uniform in our study. Most of them had a regular round shape, while some bigger and brighter particles with irregular shape were also observed in the cell (Fig. 2C). These larger particles may contain multiple RNA molecules or multi-copies of GFP

molecules. Thus for quantitative analysis, a threshold for the particle size and intensity was set up to gate single positive particles. White dots represent bright individual GFP particles (Fig. 2B), that were tracked by Imaris software in terms of the particle number and intensity.

Visualization of IL-6 Transcription Activity

By monitoring the accumulation and intensity of the MS2-GFP fusion protein particles, we can visualize dynamic activation of IL-6 transcription following IL-1 α treatment in single cells with great sensitivity. As shown in Figure 3C, IL-6 transactivation is evident within 60 min (started at 30 min, data is not shown) after IL-1 α treatment, then the number of the GFP particles dramatically increase and then continue to accumulate throughout the whole imaging time (up to 400 min) without interruption.

Verification of MS2-GFP System

To verify the MS2-GFP system, flow cytometry was used to detect the expression of RFP and GFP in NP cells after transfection ($n=3$). The RFP and

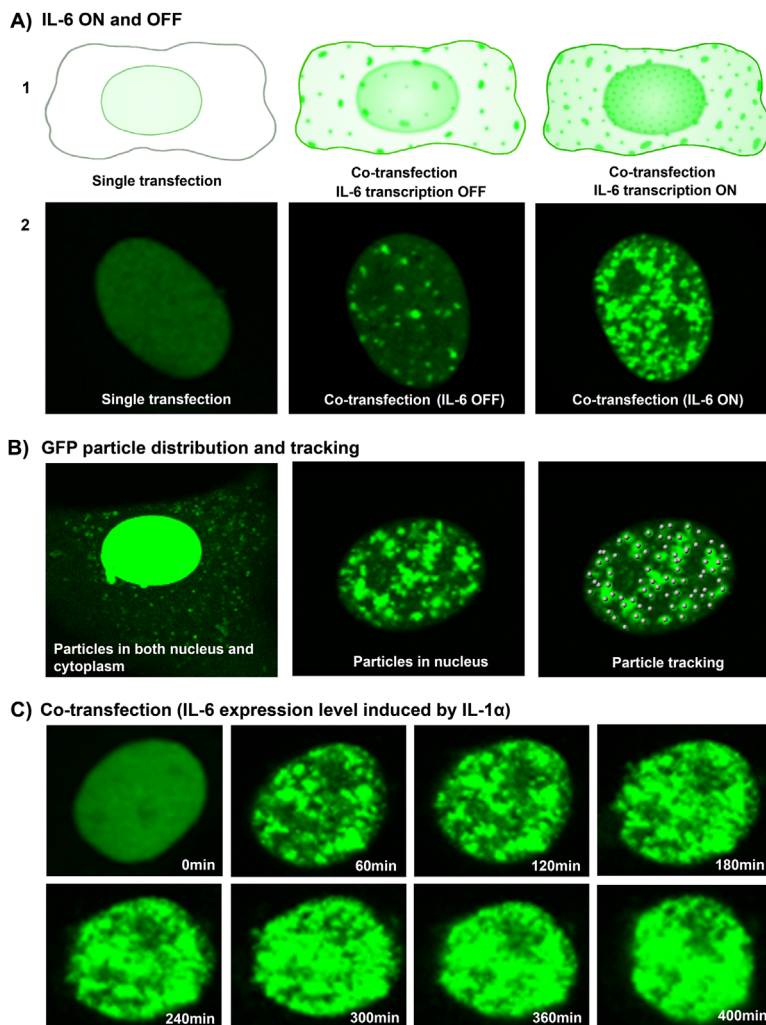
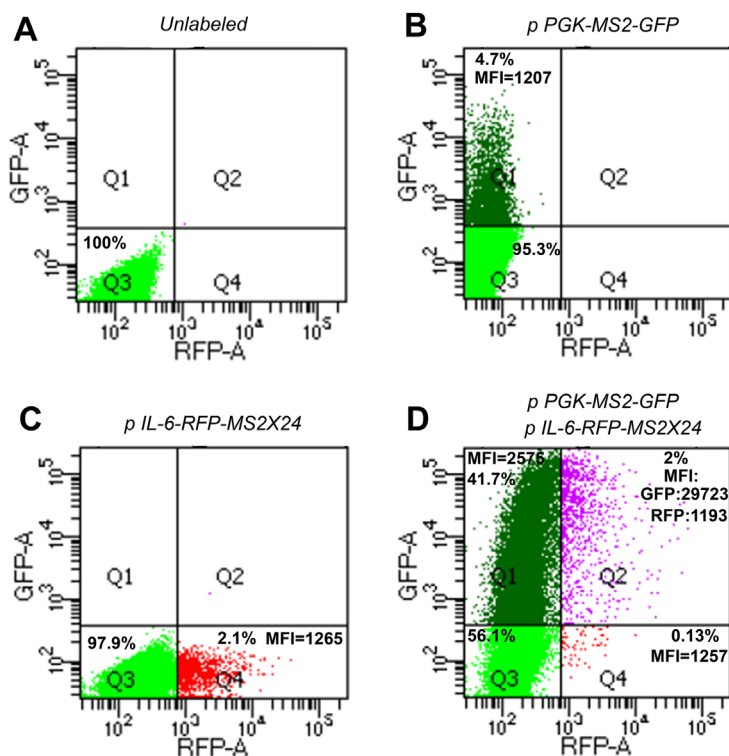


Figure 2. Visualization of dynamic mRNA expression in individual live cells. A1) Illustration of IL-6 expression ON and OFF in MS2-GFP system. A2) Single GFP particles in living cells after transfection. B) GFP particle distribution in single living cells after co-transfection (both in the cytoplasm and nucleus); White dots represent GFP particles that are tracked with Imaris software. C) Dynamic imaging of GFP in nucleus of living cells after co-transfection (induced by IL-1 α) for 400 min. Exposure time is reduced to visualize the particulate nature of the intense nuclear stain.



p PGK-MS2-GFP/ p IL-6-RFP-MS2X24 co-transfection

Quadrant	Positive percentage	Median intensity
Q1	41.7%±12%	GFP: 2576±1285
Q2	2%±1.0%	GFP: 29723±12341 RFP: 1193±583
Q4	0.13%±0.06%	RFP: 1257±382

Figure 3. Flow cytometry verifying the GFP and RFP profile in MS2-GFP fusion and mRNA reporter system. A) Control, without transfection. B) MS2-GFP fusion plasmid single transfection C) IL-6-RFP-MS2 plasmid single transfection D) Co-transfection ($n = 3/\text{group}$). MFI = mean fluorescence intensity.

GFP labeled cell populations were delineated with quadrants data (Fig. 4). About 4.7% of plasmid A-transfected cells were GFP-positive (Fig. 3B), 2.1% of plasmid B-transfected cells were RFP-positive (Fig. 3C), and 2% of co-transfected cells were double labeled with both RFP and GFP (Fig. 3D). The intensity and number of GFP-positive cells were dramatically increased in the co-transfection group compared with the single transfection group (increased from 4.7%, MFI 1207 (Fig. 3B) up to 41.7%, MFI 2575 (Fig. 3D), MFI = mean fluorescence intensity), which corresponded to the specific binding of MS2-GFP fusion protein to the MS2 mRNA repeat sequences, which amplifies the GFP signal. Flow cytometry data confirmed that RFP signals were detected both in IL-6-MS2 mRNA reporter transfected cells and co-transfected cells; interestingly, GFP signals were significantly amplified in co-transfected cells, which was consistent with the schematics and imaging data in Figures 1 and 2.

Dynamic Imaging of IL-1 α and PEMF Effects on IL-6 Gene Transcription

Time-lapse imaging demonstrated the dynamic regulation of GFP particle number and intensity in response to IL-1 α and PEMF treatment from 0 min to 6 h (Fig. 4). Three cells were selected as representative images of each the DMEM Basal Medium group, IL-1 α treatment group, and IL-1 α + PEMF group, respectively. No bright GFP particles were found at the beginning of imaging in all cells (0 min) except for some diffuse green fluorescence in nucleus. Soon after IL-1 α treatment, bright GFP particles appeared. Although the timing varies slightly among cells, this increase is consistently observed 30 min after IL-1 α stimulation and continue to increase over time. In DMEM Basal Medium, the GFP levels representing IL-6 expression were obviously lower than in the IL-1 α treated group throughout the experiment (Fig. 4). However, in the IL-1 α treatment group, a dramatic increase was observed in both GFP intensity and particle number as early as 30 min. This signal peaks

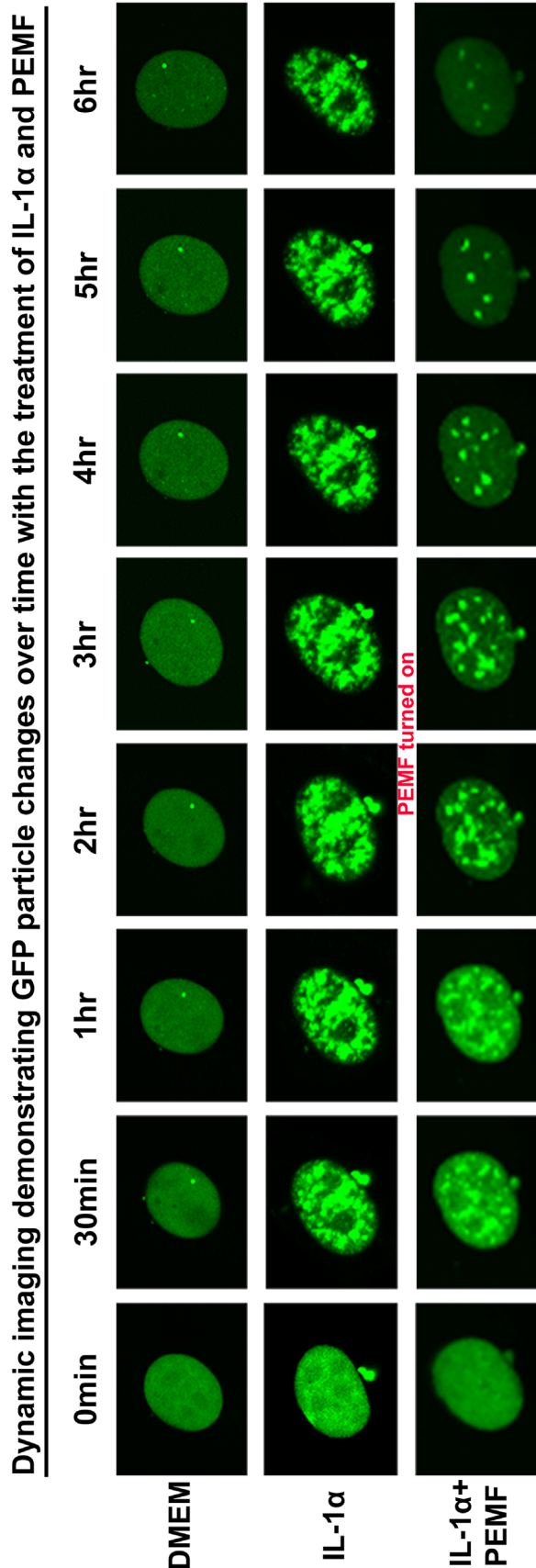


Figure 4. Dynamic images demonstrating the effects of IL-1 α alone and IL- α +PEMF treatment on IL-6 expression. PEMF dosing started at 2h after IL-1 α treatment.

at about 1–2h and is maintained for up to 6.5h without interruption. As a result, the nucleus turned exceedingly green due to the aggregation of the bright GFP particles.

Interestingly, GFP expression showed a significant change after PEMF treatment. PEMF was applied 2h after IL-1 α induction. Prior to PEMF stimulation, IL-1 α increased GFP particle levels to a peak at 2h. Rapidly after PEMF treatment, MS2-GFP particle numbers and intensity rapidly returned to basal levels, with an initial decrease observed 30 min post-PEMF (around 2.5 h), and a sharp reduction apparent from 4 to 6 h.

Quantification of PEMF Treatment Effects on IL-6 Expression

The GFP particle number and intensity were tracked with the tracking module of Imaris software ($n = 9$ for each group). Consistent with the qualitative analysis of the GFP images, this quantitative approach showed that IL-6 is expressed at a low basal level in the DMEM group, while it was activated significantly by IL-1 α treatment within 30 min and peaked at about 1–2h, then maintained to 6 h ($p < 0.01$). However, the inductive effects of IL-1 α were inhibited by PEMF treatment significantly as early as 2h ($p < 0.01$), and GFP particle number continuously decreased until 6.5 h. By 3.5 h, there was no significant difference between the IL-1 α +PEMF treated cells and the DMEM Basal Medium group (Fig. 5). The quantification results matched the imaging data shown in Figure 4.

Real-Time PCR Validation of PEMF Effects on IL-6 Expression Induced by IL-1 α

To further verify these results, which are based on single cell dynamic imaging analysis, we assessed gene expression at the population level using qRT-PCR. IL-6 is expressed at low levels in DMEM

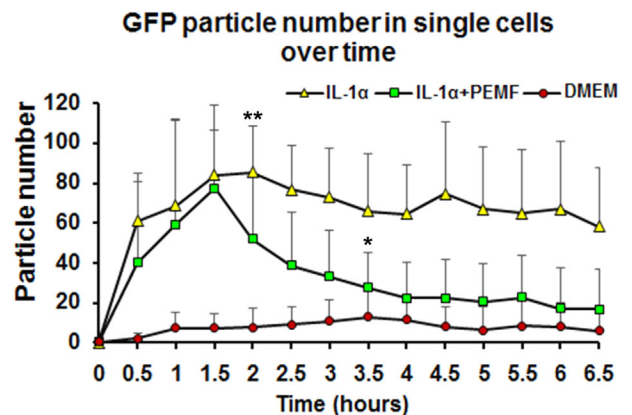


Figure 5. Quantification of IL-1 α and PEMF treatment effects by calculating GFP particle number over time ($n = 9$ /group). PEMF dosing started at 2h after IL-1 α treatment (blue arrow) and turned off at 6h (red arrow). Significant differences between IL-1 α and IL-1 α +PEMF group starts at 2hr ($p < 0.01$). Loss of significance occurred between IL- α +PEMF and DMEM groups at 3.5h ($p < 0.05$).

Basal Medium within 48 h. After treatment with IL-1 α , IL-6 expression tended to increase starting from 3 h ($p=0.07$) and continuously went up in a time-dependent manner over time (up to 8 h) (Fig. 6) ($p < 0.01$). However, this inductive effect of IL-1 α on IL-6 expression was significantly reduced around 8 h ($p < 0.01$). PEMF treatment did not induce any pre-apoptosis cell response or toxic effects as detected in a live/dead assay.³⁵

DISCUSSION

Pro-inflammatory cytokines play a predominant role during disc degeneration by inducing catabolic proteases, which drive extracellular matrix degeneration.^{6,7} We previously showed that IL-1 α induces the expression of IL-6 and catabolic protease levels in nucleus pulposus cells in 3D culture, and PEMF treatment inhibited this upregulation induced by IL-1 α after 4 days culture.³⁵ These data suggested that PEMF can repress inflammatory responses that play a causal role in musculoskeletal tissue degeneration. To investigate the mechanisms of PEMF action in more detail, it is essential to understand the dynamic effects of PEMF on transcription with greater temporal and spatial resolution (Fig. 5).

In this current study, we present a validated MS2-GFP reporter system to dynamically visualize the regulation of IL-6 transcription under an inflammation and PEMF treatment conditions. This system detects the ability of IL-1 α to rapidly trigger IL-6 transcription and to maintain this expression continuously over several hours, which is consistent with previous data that IL-1 could up-regulate IL-6 expression during disc degeneration^{7,35} as well as in the validation studies presented here (Figs. 2 and 4). This system also provides dynamic high-resolution insight into the effects of IL-1 α and PEMF on IL-6 transactivation. Quantitative analysis of GFP particle number confirmed the imaging visualization (Fig. 5). Dynamic images illustrated the process that PEMF treatment rapidly repressed the inductive effects of IL-1 α on IL-6

expression by decreasing GFP particle number as early as 0.5 h after PEMF dosing. It suggests that PEMF treatment regulates inflammatory responses associated with disc degeneration. Given the immediate early response of PEMF in repressing IL-6 transcription, it raises questions about the mechanisms of PEMF action. Future studies can explore those potential regulation of inflammatory pathways. For example, recent studies implicated NF-kappa B (NF- κ B), p38 mitogen-activated protein kinase (MAPK), calcium ATPase or adenylate cyclase receptor, and nitric oxide signaling are involved in cartilage inflammation and skeletal tissue degeneration, which suggested that these pathways may potentially participate in the mechanism of PEMF action on inflammation.^{32,33,48,49} In addition, previous work showed that PEMF action increased basal levels of Ca²⁺ and calcineurin activity in osteoblasts.⁵⁰ It is unclear if PEMF action would affect Ca²⁺ activity, which could potentially influence the MS2-GFP reporter system used in our current study. However, we do not expect that this is a problem since previous work has shown that the GFP-MS2 system is very stable owing to the strong and unique affinity between MS2 protein and the MS2 binding site. It would be interesting to elucidate the role of downstream effectors in PEMF treatment on disc inflammation in future studies. We are currently exploring the mechanisms of PEMF action, including the involvement of the NF- κ B, MAPK, and Ca²⁺ signaling pathways. Furthermore, more and more studies have been trying to find the mechanical modulation of cell, tissue, and organ functions in the field of mechanobiology. The MS2-GFP reporter system is a promising tool that can be applied to visualize the dynamic modulation of mechanobiologic mechanisms in single living cells.

It is worth noting that, this novel IL-6 MS2-GFP reporter system can detect the effects of PEMF on IL6 expression more rapidly and with greater sensitivity than traditional approaches. It provided us a visualization of dynamic transactivation of IL-6 mRNA at temporal and spatial resolution in single living cells during IL-1 α and IL-1 α + PEMF treatment. Compared with standard methods such as qRT-PCR or in situ hybridization that are limited to detect gene expression in cell population or fixed cells, the MS2-GFP reporter system could be invaluable in elucidating and quantifying the real time effects of PEMF treatment on inflammation. It could also be applied broadly in other cell types and in other clinical scenarios to investigate the dynamic regulation of IL-6 in many circumstances. However, there are some limitations about this system. It is difficult to monitor the particles both in the nucleus and cytoplasm simultaneously due to the extremely strong fluorescence intensity in the nucleus compared to the cytoplasm (Fig. 3B). Therefore, the current experiment focused on nucleoplasm. We used the Mark and Find function of confocal microscope to select and measure as many

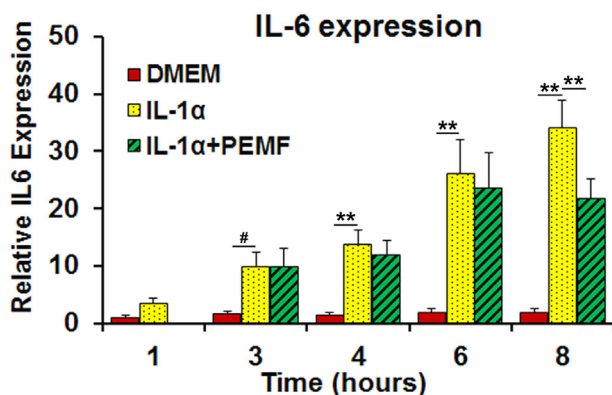


Figure 6. Real time RT-PCR validation for PEMF and IL-1 α treatment effects. # represents $p=0.07$; ** represents $p < 0.01$. $n=3$ for biological replicates and $n=3$ technical replicates.

cells as possible within a reasonable timeframe. It is hard to extract the whole cell information from multiple cells in a single image stack since the cells are not exactly at the same focal plane. Therefore, we did three experiment replicates to minimize the potential source bias. Additionally, the signal for RFP (red fluorescent protein) that was used to screen positive cells in the IL-6-MS2 mRNA reporter, unfortunately, was too weak to be observed with microscopy. It could be that the intensity of a single RFP molecule is weak, and it does not have the accumulative or amplified effect observed for GFP when GFP-MS2-binding sites group after the transcripts are transported back to nucleus. Furthermore, singly transfected cells did not show a very high intensity owing to the single molecule GFP or RFP. For that reason, flow cytometry was performed to validate the reporter system instead, which demonstrated the effectiveness of the reporter system used in our study. Due to the large plasmid size and the unsynchronized primary cells, the transfection efficiency was not high. However, the consistent positive population in multiple replicates in this experiment supported the stability and effectiveness of this system during these experiments. Also, in this system, the non-uniform distribution of RNA molecules which form GFP particles and the changing focal plane of particle location and unsynchronized primary cells may cause variations of the particle number and intensity among individual cells in imaging. Although variations existed in the exact time up- or down-regulation, both PCR and imaging demonstrated that PEMF treatment could inhibit IL-6 expression in nucleus pulposus cells. The overall trends are the same at the gene and protein level. Thus, this MS2-GFP system is an effective tool for visualizing dynamic IL-6 transcription regulation during disc degeneration therapy such as PEMF treatment. For recapitulating physiological conditions that are more clinically relevant, PEMF treatment will be applied in explant or organ culture model. Most importantly, it also could be a promising tool for treatment screening and optimization for other musculoskeletal disease therapy.

CONCLUSION

Dynamic imaging of mRNA transcription demonstrated the inhibitory effects of PEMF treatments on IL-6 transcription induced by pro-inflammatory factor IL-1 α . The results indicated that PEMF treatment could be used as a potential therapy to protect tissue from the high inflammatory cytokine environment during disc degeneration. We also show that the MS2-tagged GFP reporter system is a promising tool for sensitively tracking mRNA transcription in individual cells, which could be used for investigating biological and pathological mechanisms associated with disc degeneration, and for optimizing therapies such as

PEMF for the treatment of low back pain and other musculoskeletal diseases. The MS2-GFP reporter system is a promising tool to visualize mechanotransduction with high spatiotemporal resolution in living cells in musculoskeletal research.

AUTHORS' CONTRIBUTIONS

This study was designed by Jeffery Lotz, Tamara Alliston, Dezba Coughlin and Xinyan Tang. Data were collected and analyzed by Xinyan Tang and Stephanie Miller, data interpreted by all authors; the manuscript was drafted by Xinyan Tang, and revised by Jeffery Lotz, Tamara Alliston, Dezba Coughlin, Nianli Zhang, Erik I Waldorff and James T Ryaby. All authors approve the final submitted version.

ACKNOWLEDGMENT

This research was supported by Orthofix Inc., Lewisville, Texas.

REFERENCES

1. Katz JN. 2006. Lumbar disc disorders and low-back pain: socioeconomic factors and consequences. *J Bone Joint Surg Am* 88:21–24.
2. Hoy D, March L, Brooks P, et al. 2010. The global burden of low back pain: estimates from the Global Burden of Disease study. *Ann Rheum Dis* 73:968–974.
3. Martin BI, Deyo RA, Mirza SK, et al. 2008. Expenditures and health status among adults with back and neck problems. *JAMA* 299:656–664.
4. Kao TH, Peng YJ, Tsou HK, et al. 2014. Nerve growth factor promotes expression of novel genes in intervertebral disc cells that regulate tissue degradation: laboratory investigation. *J Neurosurg Spine* 21:653–661.
5. Yurube T, Takada T, Suzuki T, et al. 2012. Rat tail static compression model mimics extracellular matrix metabolic imbalances of matrix metalloproteinases, aggrecanases, and tissue inhibitors of metalloproteinases in intervertebral disc degeneration. *Arthritis Res Ther* 14:R51.
6. Mern DS, Beierfuß A, Fontana J, et al. 2014. Imbalanced protein expression patterns of anabolic, catabolic, anti-catabolic and inflammatory cytokines in degenerative cervical disc cells: new indications for gene therapeutic treatments of cervical disc diseases. *PLoS ONE* 9:e96870.
7. Le Maitre CL, Freemont AJ, Hoyland JA. 2005. The role of interleukin-1 in the pathogenesis of human intervertebral disc degeneration. *Arthritis Res Ther* 7:R732–R745.
8. Sakai D, Andersson GB. 2015. Stem cell therapy for intervertebral disc regeneration: obstacles and solutions. *Nat Rev Rheumatol* 11:243–256.
9. Illien-Jünger S, Sedaghatpour DD, Laudier DM, et al. 2016. Development of a bovine decellularized extracellular matrix-biomaterial for nucleus pulposus regeneration. *J Orthop Res* 34:876–888.
10. Altun I. 2016. Cytokine profile in degenerated painful intervertebral disc: variability with respect to duration of symptoms and type of disease. *Spine J* 16:857–861.
11. Gabr MA, Jing L, Helbling AR, et al. 2011. Interleukin-17 synergizes with IFN γ or TNF α to promote inflammatory mediator release and intercellular adhesion molecule-1 (ICAM-1) expression in human intervertebral disc cells. *J Orthop Res* 29:1–7.

12. Kang JD, Stefanovic-Racic M, McIntyre LA, et al. 1997. Toward a biochemical understanding of human intervertebral disc degeneration and herniation – Contributions of nitric oxide, interleukins, prostaglandin E-2, and matrix metalloproteinases. *Spine* 22:1065–1073.
13. Risbud MV, Shapiro IM. 2014. Role of cytokines in intervertebral disc degeneration: pain and disc content. *Nat Rev Rheumatol* 10:44–56.
14. Studer RK, Vo N, Sowa G, et al. 2011. Human nucleus pulposus cells react to IL-6: independent actions and amplification of response to IL-1 and TNF-alpha. *Spine (Phila Pa 1976)* 36:593–599.
15. Phillips KL, Cullen K, Chiverton N, et al. 2015. Potential roles of cytokines and chemokines in human intervertebral disc degeneration: interleukin-1 is a master regulator of catabolic processes. *Osteoarthritis Cartilage* 23:1165–1177.
16. Gruber HE, Hoelscher GL, Ingram JA, et al. 2013. Increased IL-17 expression in degenerated human discs and increased production in cultured annulus cells exposed to IL-1 α and TNF-alpha. *Biotech Histochem* 88:302–310.
17. Tian Y, Yuan W, Fujita N, et al. 2013. Inflammatory cytokines associated with degenerative disc disease control aggrecanase-1 (ADAMTS-4) expression in nucleus pulposus cells through MAPK and NF-kappaB. *Am J Pathol* 182:2310–2321.
18. Gu SX, Li X, Hamilton JL, et al. 2015. MicroRNA-146a reduces IL-1 dependent inflammatory responses in the intervertebral disc. *Gene* 555:80–87.
19. Foley KT, Mroz TE, Arnold PM, et al. 2008. Randomized, prospective, and controlled clinical trial of pulsed electromagnetic field stimulation for cervical fusion. *Spine J* 8:436–442.
20. Garland DE, Moses B, Salver W. 1991. Fracture healing: long-term follow-up of fracture nonunions treated with PEMFs. *Contemp Orthop* 22:295–302.
21. Bassett CA, Mitchell SN, Gaston SR. 1982. Pulsing electromagnetic field treatment in ununited fractures and failed arthrodeses. *JAMA* 247:623–628.
22. Bagnato GL, Miceli G, Marino N, et al. 2016. Pulsed electromagnetic fields in knee osteoarthritis: a double blind, placebo-controlled, randomized clinical trial. *Rheumatology* 55:755–762.
23. Androjna C, Fort B, Zborowski M, et al. 2014. Pulsed electromagnetic field treatment enhances healing callus biomechanical properties in an animal model of osteoporotic fracture. *Bioelectromagnetics* 35:396–405.
24. De Mattei M, Pasello M, Pellati A, et al. 2003. Effects of electromagnetic fields on proteoglycan metabolism of bovine articular cartilage explants. *Connect Tissue Res* 44:154–159.
25. Chalidis B, Sachinis N, Assiotis A, et al. 2011. Stimulation of bone formation and fracture healing with pulsed electromagnetic fields: biologic responses and clinical implications. *Int J Immunopathol Pharmacol* 24:17–20.
26. Liu M, Lee C, Laron D, et al. 2017. Role of pulsed electromagnetic fields (PEMF) on tenocytes and myoblasts – potential application for treating rotator cuff tears. *J Orthop Res* 35:956–964.
27. Sun LY, Hsieh DK, Lin PC, et al. 2010. Pulsed electromagnetic fields accelerate proliferation and osteogenic gene expression in human bone marrow mesenchymal stem cells during osteogenic differentiation. *Bioelectromagnetics* 31:209–219.
28. de Girolamo L, Stanco D, Galliera E, et al. 2013. Low frequency pulsed electromagnetic field affects proliferation, tissue-specific gene expression, and cytokines release of human tendon cells. *Cell Biochem Biophys* 66:697–708.
29. Okada M, Kim JH, Hutton WC, et al. 2013. Upregulation of intervertebral disc-cell matrix synthesis by pulsed electromagnetic field is mediated by bone morphogenetic proteins. *J Spinal Disord Tech* 26:167–173.
30. Gómez-Ochoa I, Gómez-Ochoa F, Gómez-Casal F, et al. 2011. Pulsed electromagnetic fields decrease proinflammatory cytokine secretion (IL-1 β and TNF-alpha) on human fibroblast-like cell culture. *Rheumatol Int* 31:1283–1239.
31. Varani K, Padovan M, Vincenzi F, et al. 2011. A2A and A3 adenosine receptor expression in rheumatoid arthritis: upregulation, inverse correlation with disease activity score and suppression of inflammatory cytokine and metalloproteinase release. *Arthritis Res Ther* 13:R197.
32. Vincenzi F, Targa M, Corciulo C, et al. 2013. Pulsed electromagnetic fields increased the anti-inflammatory effect of A(2)A and A(3) adenosine receptors in human T/C-28a2 chondrocytes and hFOB 1.19 osteoblasts. *PLoS ONE* 8:p.e65561.
33. Selvam R, Ganesan K, Narayana Raju KV, et al. 2007. Low frequency and low intensity pulsed electromagnetic field exerts its antiinflammatory effect through restoration of plasma membrane calcium ATPase activity. *Life Sci* 80:2403–2410.
34. Reihani Kermani H, Pourghazi M, Mahani SE. 2014. Effects of pulsed electromagnetic field on intervertebral disc cell apoptosis in rats. *Electromagn Biol Med* 33:246–249.
35. Miller SL, Bradshaw R, Coughlin DG, et al. 2016. Pulsed electromagnetic field (PEMF) treatment reduces expression of genes associated with disc degeneration in human intervertebral disc cells. *Spine J* 16:770–776.
36. Bertrand E, Chartrand P, Schaefer M, et al. 1998. Localization of ASH1 mRNA particles in living yeast. *Mol Cell* 2:37–45.
37. Fusco D, Accornero N, Lavoie B, et al. 2003. Single mRNA molecules demonstrate probabilistic movement in living mammalian cells. *Curr Biol* 13:161–167.
38. Zenklusen D, Wells AL, Condeelis JS, et al. 2007. Imaging real-time gene expression in living yeast. *CSH Protoc* pdb. prot 4870. <https://doi.org/10.1101/pdb.prot4870>
39. Querido E, Chartrand P. 2008. Using fluorescent proteins to study mRNA trafficking in living cells. *Methods Cell Biol* 85:273–292.
40. Häkkinen A, Kandhavelu M, Garasto S, et al. 2014. Estimation of fluorescence-tagged RNA numbers from spot intensities. *Bioinformatics* 30:1146–1153.
41. Yunger S, Rosenfeld L, Garini Y, et al. 2010. Single-allele analysis of transcription kinetics in living mammalian cells. *Nat Methods* 7:631–633.
42. Yunger S, Rosenfeld L, Garini Y, et al. 2013. Quantifying the transcriptional output of single alleles in single living mammalian cells. *Nat Protoc* 8:393–408.
43. Halstead JM, Lionnet T, Wilbertz JH, et al. 2015. Translation, An RNA biosensor for imaging the first round of translation from single cells to living animals. *Science* 347:1367–1371.
44. Femino AM, Fay FS, Fogarty K, et al. 1998. Visualization of single RNA transcripts in situ. *Science* 280:585–590.
45. Livak KJ, Schmittgen TD. 2001. Analysis of relative gene expression data using real-time quantitative PCR and the 2^{-Delta Delta C (T)} Method. *Methods* 25:402–408.
46. Wilkie GS, Davis I. 2001. Drosophila wingless and pair-rule transcripts localize apically by dynein-mediated transport of RNA particles. *Cell* 105:209–219.
47. Kloc M, Zearfoss NR, Etkin LD. 2002. Mechanisms of subcellular mRNA localization. *Cell* 108:533–544.
48. Sanchavanakit N, Saengtong W, Manokawinchoke J, et al. 2015. TNF- α stimulates MMP-3 production via PGE2 signaling through the NF-kB and p38 MAPK pathway in a murine cementoblast cell line. *Arch Oral Biol* 60:1066–1074.

49. Tisherman R, Coelho P, Phillibert D, et al. 2016. NF- κ B signaling pathway in controlling intervertebral disk cell response to inflammatory and mechanical stressors. *Phys Ther* 96:704–711.
50. Zhang J, Xu H, Han Z, et al. 2017. Pulsed electromagnetic field inhibits RANKL-dependent osteoclastic differentiation in RAW264.7 cells through the Ca²⁺ + –calcineurin-NFATc1

signaling pathway. *Biochem Biophys Res Commun* 482: 289–295.

SUPPORTING INFORMATION

Additional supporting information may be found in the online version of this article.